JOURNAL OF MATERIALS SCIENCE 30 (1995) 904–915

The crystallization kinetics of a glass based on the cordierite composition studied by DTA and DSC

I. W. DONALD
Atomic Weapons Establishment, Aldermaston, Berkshire, UK

The crystallization kinetics of a glass based on the cordierite composition have been studied by DTA and DSC. Crystallization has been observed to be very dependent on the particle size of the glass employed, indicating a strong dependence on surface crystallization. For coarse particle sizes (eg. 600–1000 μm) a single crystallization exotherm is obtained, corresponding to the formation of α-cordierite. For smaller particle sizes (eg ≤ 212 μm) two distinct crystallization exotherms are resolved corresponding to the initial formation of metastable μ-cordierite, followed by its transformation at higher temperatures to the α-cordierite phase. Activation energies for crystallization have been determined for different particle sizes of glass using a number of isothermal and non-isothermal methods, and the results compared. In general, agreement between DTA and DSC, and the various methods employed, is good, although the isothermal methods appear to reflect more strongly the *early* crystallization processes, i.e. they relate more closely to the activation energy for the formation of the μ-cordierite phase. A value for the activation energy corresponding to structural relaxation at temperatures around the glass transition has also been determined for this cordierite glass.

1. Introduction

Cordierite glass-ceramics are interesting candidates for a number of elevated temperature applications where good high temperature creep resistance coupled with a high resistance to thermal shock are required [1–3]. These materials are, however, difficult to prepare using conventional glass-ceramic techniques because of the refractory nature of the starting glasses. Attempts at using sintering routes employing glass powders as the starting material have therefore been reported [4–17]. Unfortunately, success has been limited because surface crystallization of the powders occurs, which inhibits the sintering process, before adequate densification has taken place. Although sintering performance can be improved by incorporation of suitable fluxing agents, eg. B_2O_3 or P_2O_5, or by using MgO-Al_2O_3-SiO_2 glass compositions of lower softening point than stoichiometric cordierite, the high temperature properties of the resulting glass-ceramics are normally impaired. Ideally, for the preparation of refractory cordierite glass-ceramics of near theoretical density, surface crystallization needs to be suppressed, whilst controlled bulk crystallization of a densified compact should be enhanced. It is therefore important, in the first instance, to gain a thorough understanding of the processes involved in the crystallization of these materials. Although a number of studies have been reported aimed specifically at examining the sintering and/or crystallization mechanisms of cordierite-based glasses [4–23], and in determining the kinetic parameters [24–29], a more comprehensive data base is required before a clearer understanding of the crystallization processes can emerge. In the present investigation, the crystallization kinetics of a magnesium aluminosilicate glass of composition close to that of stoichiometric cordierite were examined by differential thermal analysis (DTA) and differential scanning calorimetry (DSC). The results are reported and discussed in this paper.

2. Glass composition and preparation

The composition of the glass used in the present investigation is given in Table I. The glass was prepared at Schott Glaswerke, Mainz, Germany, by melting the constituent oxides in a 30 l Pt pot for 1 h at 1700 °C. Due to the low viscosity of the glass at this temperature, homogenization occurs by convection without stirring. Thin glass ribbons were produced directly from material held in the pot by quenching through cooled rollers; these ribbons were used in the as-received, un-annealed state for the present DTA and DSC investigations. Due to the influence of thermal shock during production, the ribbons were received in the form of small crazed pieces which were easily broken into small particles. The work currently reported was performed using ribbon from a single melt.

0022–2461

TABLE I Composition of the glass used in the present investigation

	MgO (wt %)	Al_2O_3 (wt %)	SiO_2 (wt %)
Analysed composition	14.6	33.2	52.3
Stoichiometric cordierite	13.78	34.86	51.36

3. Thermal analysis investigations

3.1. Sample preparation

The as-received broken glass ribbons were lightly crushed and then sieved to produce different size fractions of "as-quenched" glass powder suitable for DTA and DSC analysis. No further treatment was given to this glass.

3.2. Differential thermal analysis

Differential thermal analysis was performed employing a Stanton Redcroft DTA Model 674 with an operating capability in air covering the range ambient to 1500 °C. The sample glass of weight 160 ± 5 mg was contained in a Pt crucible. Alumina contained in a Pt crucible was employed as the reference material. The data were recorded by means of a chart recorder from which temperature was measured manually.

3.3. Differential scanning calorimetry

Differential scanning calorimetry was performed employing a Netzsch DSC Model 404; this too has an operating capability in air to 1500 °C. The sample glass of weight 30 ± 1 mg was contained in a Pt pan; an empty Pt pan was used as the standard. Data were recorded using a computer-driven data acquisition system.

3.4. Calibration of DTA and DSC

3.4.1. Temperature calibration

Calibration was carried out over a range of temperatures employing high purity (99.999%) materials approved by the Committee on Standardization of the International Confederation for Thermal Analysis (ICTA) [30,31], e.g. Ag_2SO_4, SiO_2, K_2SO_4 and $BaCO_3$.

The overall accuracy of the DTA was driven by the degree of accuracy to which temperatures could be measured from the chart recorder, i.e. $\approx \pm 2$ K. Within this limitation, calibration of the DTA was relatively insensitive to absolute temperature or heating rate for rates $\leq 10\,\mathrm{K\,min^{-1}}$. For the DSC, temperature was recorded to 0.1 K, and temperature calibration was therefore more critical. Temperature calibration plots were prepared comparing the ICTA value for each calibrant as a function of the recorded instrument temperature for different heating rates. The overall accuracy of this instrument is expected to be within ± 0.5 K.

3.4.2. Heating rate calibration

Heating rate, $\dot{T}$, was controlled electronically with the DSC, and electromechanically with the DTA. The heating rate values set with the DSC were checked for accuracy by monitoring temperature as a function of time for a range of nominal heating rate values. Calibration plots of recorded heating rate as a function of measured heating rate were subsequently constructed. For the DTA, heating rate values were determined for each DTA run by measurement from the temperature chart.

3.4.3. Enthalpy calibration

The DSC was calibrated for enthalpy over a range of temperature using the same materials as were employed in the temperature calibration, together with $SrCO_3$ and Au. Appropriate literature enthalpy values were used [31]. Enthalpy measurements are expected to be accurate to within $\pm 10\%$.

4. Properties measured

4.1. Characteristic temperatures

In the present work, the temperatures associated with the glass transition, T_g, the start of crystallization, $T_{x_{(s)}}$, the extrapolated start of crystallization, $T_{x_{(es)}}$, the crystallization peak, T_p, the extrapolated end of crystallization, $T_{x_{(ee)}}$, and the end of crystallization, $T_{x_{(e)}}$, were measured. A minimum of ten samples was employed for each determination.

4.2. Nucleating efficiency

A preliminary assessment of the nucleating efficiency of a given glass system can be made using the method of Thakur and Thiagarajan [32] in which the variation in peak crystallization temperature is monitored as a function of the glass particle size. In the present work, different particle size ranges were employed (i.e. < 45 μm; 45–212 μm; 212–600 μm; 600–1000 μm; and a single piece of weight ≈ 30 mg and dimensions $\approx 3\,\mathrm{mm} \times 3\,\mathrm{mm} \times 1.3\,\mathrm{mm}$). If surface crystallization is the predominant crystallization mechanism, a strong dependence of crystallization peak temperature on particle size would be expected. If, on the other hand, bulk crystallization predominates, there should be little variation in peak temperature with particle size.

4.3 Enthalpy of crystallization

The enthalpy of crystallization of samples of the cordierite glass (weighed to an accuracy of ± 0.02 mg) was measured by peak area integration employing the DSC software. A standard particle size of 600–1000 μm was used for these determinations at a heating rate of $10\,^{\circ}\mathrm{C\,min^{-1}}$.

4.4. Optimum nucleating temperature

It is possible, using a method developed by Marotta *et al.* [33–36], to determine by thermal analysis

whether or not "nucleation" at a given temperature enhances the bulk crystallization characteristics. In this technique, the difference in peak crystallization temperature, ΔT, between as-quenched and "nucleated" glass samples, $\Delta T = T_p^0 - T_p$, is plotted against the temperature of nucleation, T_{nuc}. If nucleation is effective, a maximum in ΔT vs T_{nuc} is obtained. In the present work, a standard glass particle size of 600 to 1000 μm was employed and samples were nucleated *in situ* in the DSC for 1 h in the temperature range ≈ 860 to 960 °C. Peak crystallization temperatures were monitored by heating the samples through the crystallization range at 10 °C min^{-1}.

4.5. Activation energy for crystallization

Many different methods can be used for estimating the activation energy of a process, e.g. crystallization of a glass, but care is required in the choice of method and in the interpretation of data obtained [37–40]. It should also be noted that values determined for activation energy may be compound values (corresponding, for example, to nucleation and growth processes, or overlapping of two or more crystalline phases) rather than specific to a single process. Techniques can be broadly classified into isothermal and non-isothermal methods.

4.5.1. Isothermal methods

In general, isothermal methods are related through application of the Johnson–Mehl–Avrami transformation kinetics equation [41–45]

$$F_{xd} = 1 - \exp(-kt^n) \quad (1)$$

where F_{xd} is the fraction crystallized at a given temperature in time t; k is the reaction rate constant; and n, the Avrami exponent, is a dimensionless constant which is related to the nucleation and growth mechanisms. The reaction rate constant, k, is related to the activation energy for the process, E, through the Arrhenius temperature dependence

$$k = k_0 \exp(-E/RT) \quad (2)$$

where, k_0 is a constant; R is the universal gas constant; and T is the (isothermal) absolute temperature. Taking logs, equation [2] may be re-written as:

$$\ln(k) = \ln(k_0) - E/RT \quad (3)$$

Appropriate values of k are found experimentally by plotting the fraction crystallized, F_{xd}, against the isothermal hold time for a range of different temperatures. From these plots, the time to reach a given F_{xd} can then be found for a range of F_{xd} values. Values for k and n are then determined using the relationship (derived from Equation (1))

$$\ln\{\ln[1/(1 - F_{xd})]\} = \ln(k) + n\ln(t) \quad (4)$$

and plotting $\ln\{\ln[1/(1 - F_{xd})]\}$ against $\ln(t)$ for different temperatures. A plot of $\ln(k)$ against $1/T$ for different isothermal temperatures is subsequently used to determine a value for E.

In the present work, glass of standard particle size (600–1000 μm) was employed. The fraction crystallized was determined using the DSC from a knowledge of the mean crystallization enthalpy of the cordierite glass (section 5.3) compared with the enthalpy change accompanying the isothermal heat treatment.

Strictly speaking, this method is not necessarily valid for transformations involving nucleation and growth, including surface crystallization of glass, because it assumes that a number of conditions are satisfied, which may not always be the case. For example, it is assumed that boundary conditions can be ignored (i.e. the system is infinite), that nucleation occurs uniformly and randomly, and that growth of particles terminates at their points of mutual contact but continues unrestricted elsewhere [37–40]. In the present work, only values corresponding to a limited range of F_{xd} were employed, e.g. $F_{xd} = 0.2$–0.5. This helps to minimize the influence of complicating factors which occur during the early and later stages of crystallization, e.g. in particular, restriction of crystal growth by the finite size of the glass particles.

It has been suggested that a value for the activation energy for crystallization can also be determined using data relating the time required to crystallize a given fraction of glass, e.g. $F_{xd} = 0.5$, as a function of the temperature, using the expression [46]

$$d(\ln t_{1/2})/d(1/T) = E/nR \quad (5)$$

From the slope of a plot of $\ln(t_{1/2})$ against $1/T$, the value of E/n can be found.

4.5.2. Non-isothermal methods

Apparent activation energies for crystallization may be determined employing non-isothermal methods in which some characteristic of the crystallization peak, as determined by DTA or DSC, is monitored as a function of heating rate or temperature. For example, in the modified Kissinger method, as described by Matusita *et al.* [47–49], the crystallization peak temperature is monitored as a function of the heating rate; the following relationship is then applied

$$\ln(\dot{T}^n/Tp^2) = -(mE/RT_p) + \text{constant} \quad (6)$$

where $\dot{T}$ is the heating rate, T_p is the peak crystallization temperature at a given heating rate, E is the apparent activation energy, R is the gas constant, and m and n are numerical factors which depend on the crystallization mechanism (m depends on the dimensionality of crystal growth). The parameters n and m can take on various values, as summarized in Table II. For the special case where surface crystallization is the predominant crystallization mechanism, and $m = n = 1$, Equation 1 reduces to the familiar Kissinger equation [50]. The activation energy is found from the slope $(-mE/R)$ of a plot of $\ln(\dot{T}^n/T_p^2)$ against $1/T_p$, on substitution of the appropriate values for n, m and R.

An alternative related approach [47–49] employs the modified Ozawa method using the relationship

$$\ln(\dot{T}) = -(mE/nRT_p) + \text{constant} \quad (7)$$

TABLE II Determination of the activation energies for crystallization: values for numerical parameters n and m; after Matusita *et al.* [46–48]

Crystallization mechanism	n	m
Bulk crystallization with a constant number of nuclei		
(i.e. the number of nuclei is independent of the heating rate)		
three-dimensional growth of crystals	3	3
two-dimensional growth of crystals	2	2
one-dimensional growth of crystals	1	1
Bulk crystallization with an increasing number of nuclei		
(i.e. the number of nuclei is inversely proportional to the heating rate)		
three-dimensional growth of crystals	4	3
two-dimensional growth of crystals	3	2
one-dimensional growth of crystals	2	1
Surface crystallization	1	1

Equation 7 reduces to the familiar Ozawa equation [51] for the special case of $n = m = 1$.

Another method has been employed by Marseglia [52] who has shown that a value for E/n can be found employing the relationship

$$\ln(\dot{T}/T_p) = -(E/nRT) \quad (8)$$

With the Kissinger, Ozawa and Marseglia non-isothermal approaches for determining activation energies for crystallization the deflection from the baseline is assumed proportional to the instantaneous reaction rate, i.e. at the crystallization peak temperature the reaction rates are the same, independent of the heating rate employed. This assumption requires that the temperature of the sample is uniform for all heating rates employed; fortunately, this condition can generally be met experimentally by using *small* sample sizes and *low* heating rates. In addition, the crystallization mechanism must be known so that the appropriate values for the parameters n and m can be employed in the pertinent equations. It must also be assumed that the crystallization mechanism does not change with heating rate or temperature (although if there is a significant change in mechanism, this may be reflected in the experimental data by a change in the slope of the activation energy plot).

In the present work, heating rates in the range 1 to 10 °C min^{-1} were employed with DTA, whilst rates in the range 2 to 15 °C min^{-1} were used with DSC. Corresponding sample sizes were 165 ± 5 mg for DTA, and 30 ± 1 mg for DSC (because of the smaller sample size used, higher heating rates can be employed with the DSC). A standard particle size of 600–1000 μm was used for the bulk of the work although some studies were performed using glass of finer particle size (< 45 μm and 45–212 μm), and the results compared.

4.6. Activation energy for structural relaxation

It has been proposed [53–55] that an activation energy for structural relaxation occurring around the glass transition can be found by monitoring the change in T_g with heating rate. In this method, the glass is cooled through T_g at a given cooling rate. The glass is then heated back through T_g at the same rate. This is repeated for different cooling/heating rate cycles, and the following expression employed

$$\ln(\dot{T}) \approx -E_{relax}/RT_g \quad (9)$$

The activation energy, E_{relax}, is found from the slope of a plot of $\ln(\dot{T})$ against $1/T_g$. The value obtained is expected to be related to the activation energy for viscous flow. As the glass transition occurs over a temperature range, T_g has been taken in the present work as the extrapolated start of the transition, $T_{g(es)}$, the peak of the transition, $T_{g(p)}$, and the extrapolated end of the transition, $T_{g(ee)}$. The individual values of E_{relax} obtained should be the same within experimental error (unless there is a change of mechanism within the temperature interval covered).

5. Results

5.1. Characteristic temperatures

Mean values for the characteristic temperatures of glass of standard particle size 600–1000 μm, measured by DTA nd DSC, are given in Table III. A representative DTA trace for a standard nominal heating rate of 10 °C min^{-1} is given in Fig. 1. The crystallization exotherm is characterized by a single peak with a low temperature shoulder.

5.2. Variation in peak crystallization temperature with particle size

Representative DSC plots taken for different particle size fractions of glass are given in Fig. 2. The < 45 μm and 45–212 μm size fractions exhibit two well-defined crystallization exotherms, whilst the 212–600 μm size

TABLE III Mean values for the characteristic temperatures of cordierite glass

Characteristic temperature[a]	DTA (°C)	DSC (°C)
$T_{g(es)}$	805 ± 1	805 ± 1
$T_{x(s)}$	951 ± 5	955 ± 4
$T_{x(es)}$	1031 ± 3	1023 ± 5
T_p	1077 ± 2	1071 ± 4
$T_{x(ee)}$	1099 ± 3	1096 ± 4
$T_{x(e)}$	1110 ± 7	1105 ± 3

[a] See text for details of nonmenclature (Section 4.1)

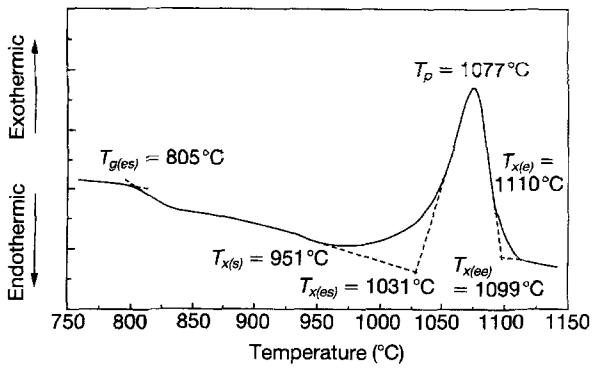

Figure 1 Representative DTA trace for cordierite glass of particle size 600–1000 μm recorded at a heating rate of 10 °C min^{-1}.

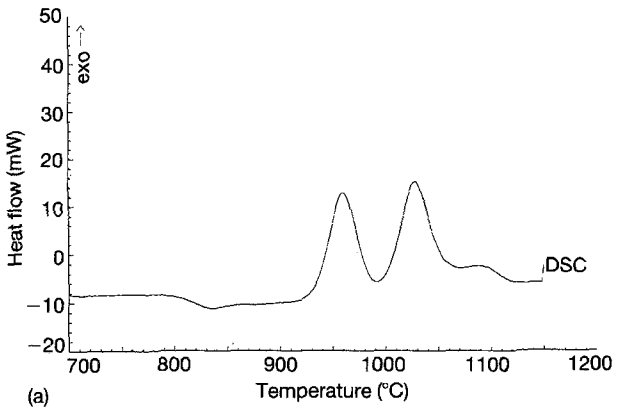

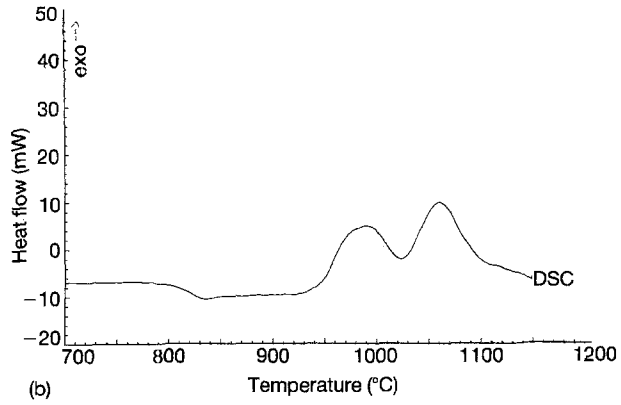

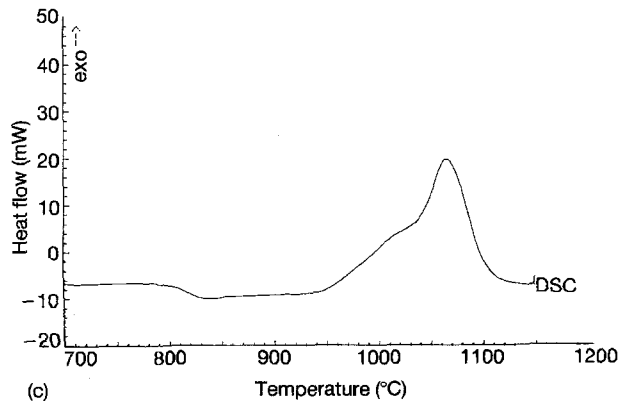

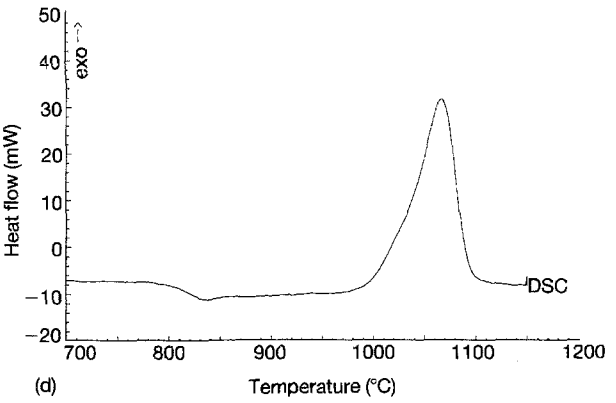

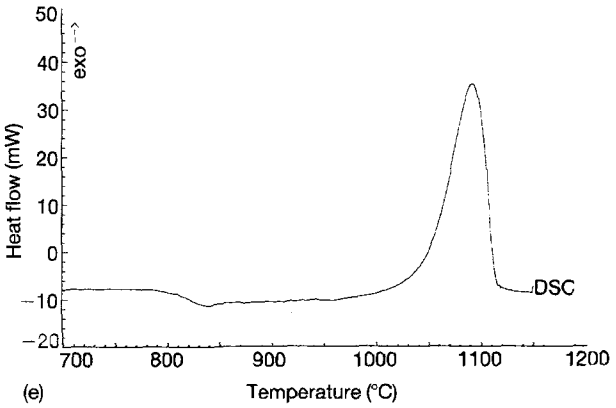

Figure 2 Representative DSC traces for cordierite glass of various particle sizes recorded at a heating rate of 10 °C min^{-1}. (a) < 45 μm; (b) 45–212 μm; (c) 212–600 μm; (d) 600–1000 μm; (e) single piece.

fraction exhibits a single peak with a well-pronounced low temperature shoulder. Individual values for the peak crystallization temperatures as a function of the particle size range employed are summarized in Table IV.

5.3. Enthalpy of crystallization

A mean value for the enthalpy of crystallization of the cordierite glass of $361.5 \pm 7\ Jg^{-1}$ was noted using DSC (10 samples).

5.4. Optimum nucleating temperature

Data showing the shift in peak crystallization temperature with "nucleation" temperature are given in Fig. 3. Crystallization enthalpy data obtained after "nucleation" are plotted in Fig. 4.

5.5. Activation energy for crystallization

5.5.1. Isothermal methods

Data for the fraction of glass crystallized, F_{xd}, as a function of the isothermal hold time at a number of different temperatures in the range 904–954 °C are plotted in Fig. 5. Information derived from these plots over the range of F_{xd} from ≈ 0.2–0.5 was employed to construct the $\ln\{\ln[1/(1 - F_{xd})]\}$ versus $\ln(t)$ plots shown in Fig. 6. These plots were subsequently used to

TABLE IV Dependence of crystallization temperature on the particle size of cordierite glass

Particle size range (μm)	$T_{x(es)}$ μ-cordierite (°C)	α-cordierite (°C)	T_p μ-cordierite (°C)	α-cordierite (°C)
< 45	934	–	961	1028
45–212	945	–	988	1060
212–600	954	1017	≈ 1012	1066
600–1000	–	1023	–	1071
single piece	–	1042	–	1091

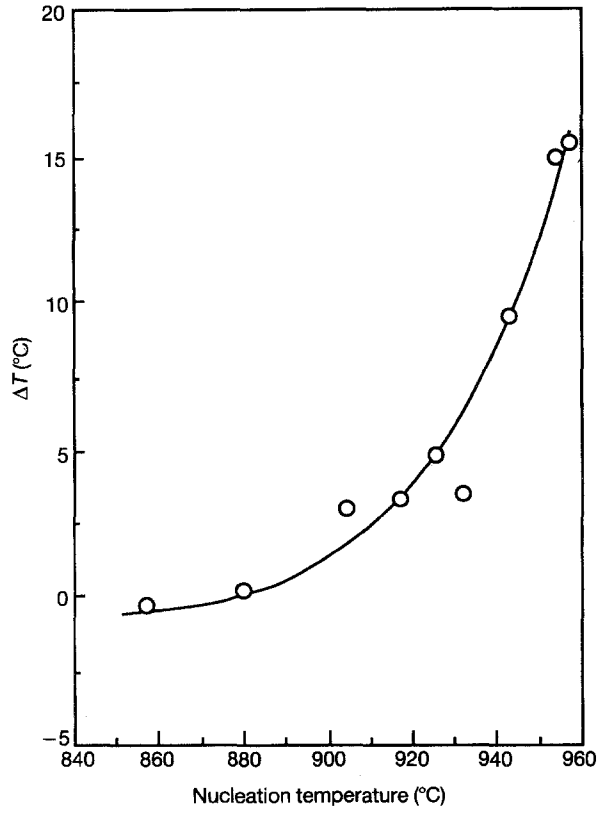

Figure 3 Variation in peak crystallization temperature between as-quenched and "nucleated" cordierite glass ($\Delta T = T_p^0 - T_p$) as a function of the temperature of "nucleation" (Marotta plot).

determine values for the reaction rate constant, k, and the Avrami exponent, n, over this range of temperature. These data, summarized in Table V, were then used to plot the graph of $\ln(k)$ versus $1/T$, shown in Fig. 7. A value of 577 kJ mol^{-1} for the activation energy of crystallization was determined from the slope of this plot.

Data were also determined for the time to reach 50% crystallinity, $t_{1/2}$, for each of the isothermal hold temperatures summarized in Table V. A plot of $\ln(t_{1/2})$ versus $1/T$ is shown in Fig. 8, from which a value for E/n of 512 kJ mol^{-1} was obtained.

5.5.2. Non-isothermal methods

Data used in the construction of non-isothermal plots for determining activation energies of crystallization

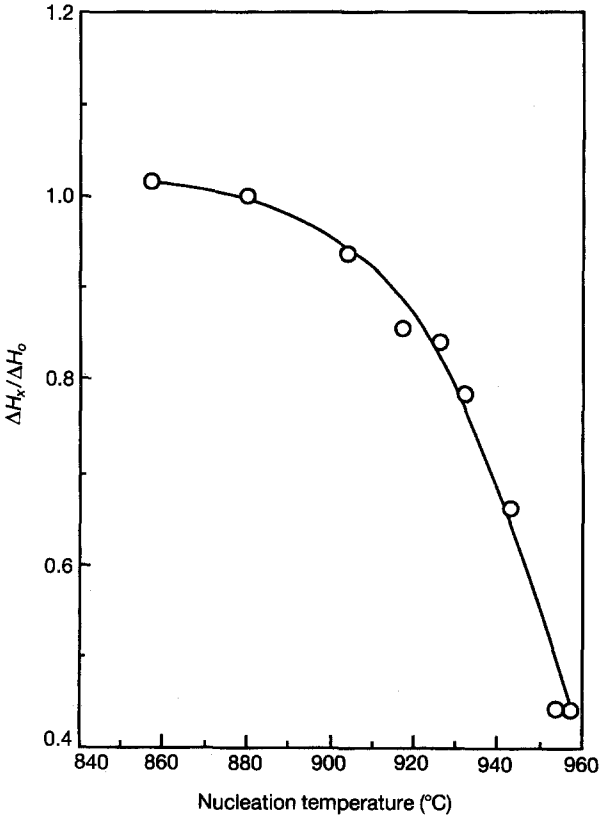

Figure 4 Normalized heat of crystallization, $\Delta H_x/\Delta H_0$, as a function of "nucleation" (isothermal hold) temperature.

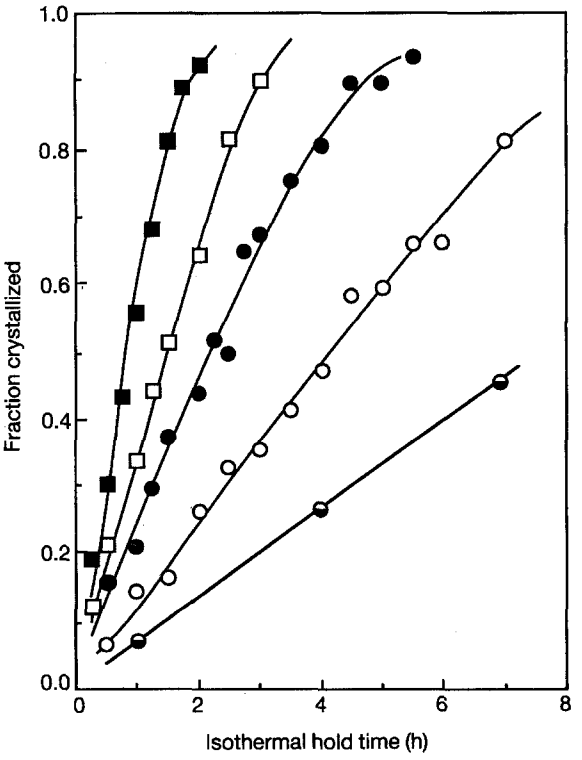

Figure 5 Plot of fraction of glass crystallized, F_{xd}, as a function of isothermal hold time for a range of temperatures. ◒, 904 °C; ○, 917 °C; ●, 932 °C; □, 943 °C; ■, 954 °C.

are summarized in Table VI–VIII. Data are included for both the DTA and DSC results. The corresponding non-isothermal activation energy plots are shown in Fig. 9–11 for the three particle sizes of glass employed, i.e. 600–1000 μm, 45–212 μm and < 45 μm. The

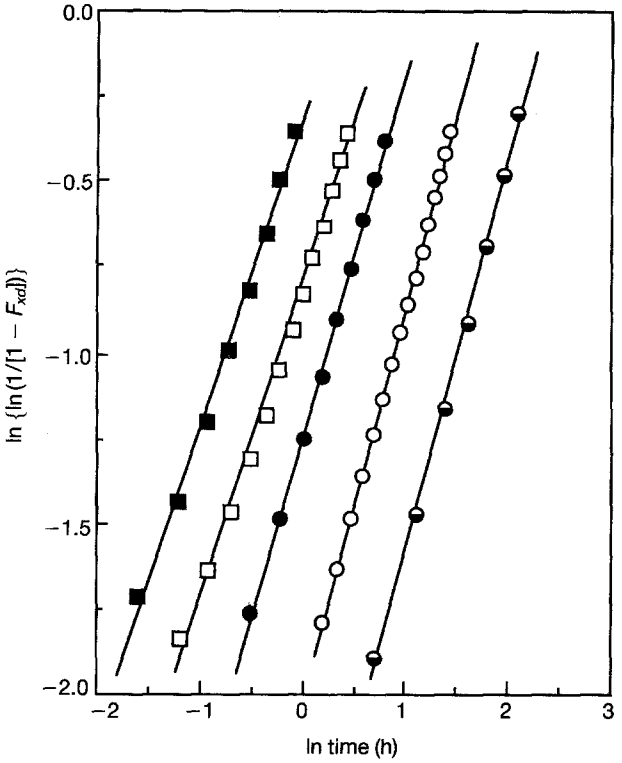

Figure 6 Plot of $\ln\{\ln[1/(1-F_{xd})]\}$ as a function of $\ln(t)$ for a range of isothermal hold temperatures. This is used in the determination of the reaction rate constant, k, and the Avrami exponent, n, for a range of temperatures. ◒, 904 °C; ○, 917 °C; ●, 932 °C; □, 943 °C; ■, 954 °C.

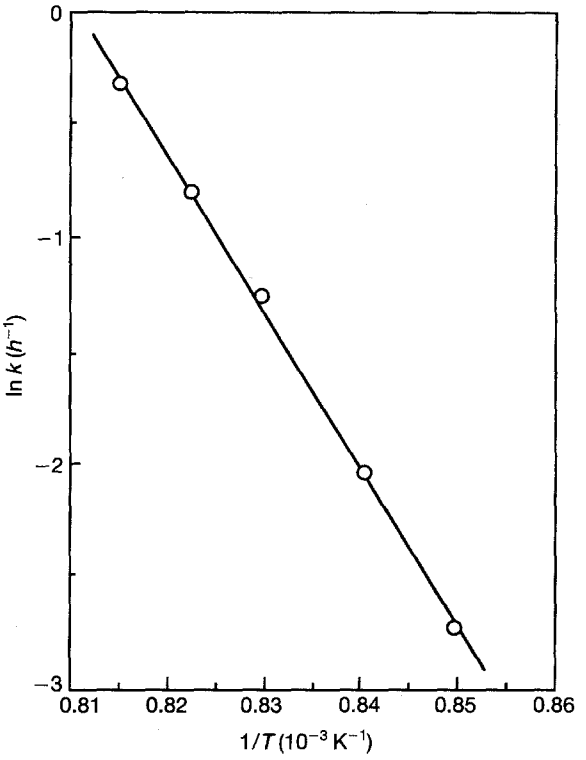

Figure 7 Plot of $\ln(k)$ against $1/T$ employed for determining the activation energy, E, of crystallization; $E = 577\ kJ\ mol^{-1}$.

TABLE V Data employed in the determination of activation energies for crystallization of cordierite glass by *isothermal* methods

Isothermal hold temperature (K)	$\ln k$ (h^{-1})	$1/T$ ($10^{-3}\,K^{-1}$)	$\ln(t_{1/2})$ (h)	n
1177	−2.717	0.8496	2.0358	1.14
1190	−2.032	0.8403	1.4387	1.15
1205	−1.246	0.8299	0.8184	1.07
1216	−0.795	0.8224	0.3874	0.93
1227	−0.323	0.8150	−0.1231	0.90

values derived for the activation energies of crystallization by the non-isothermal methods are summarized in Table IX.

5.6. Activation energy for structural relaxation

Representative DSC plots showing the glass transition region for glasses cooled and heated through T_g at different rates (e.g. 10 °C min^{-1} and 50 °C min^{-1}) are given in Fig. 12. A mean value of 766 kJ mol^{-1} for the activation energy associated with structural relaxation around T_g was determined (over the temperature range 1065–1150 °C). Individual values of 777 kJ mol^{-1} (1065–1095 °C), 765 kJ mol^{-1} (1095–1130 °C) and 756 kJ mol^{-1} (1115–1150 °C) were measured, corresponding to the extrapolated start of T_g, the peak

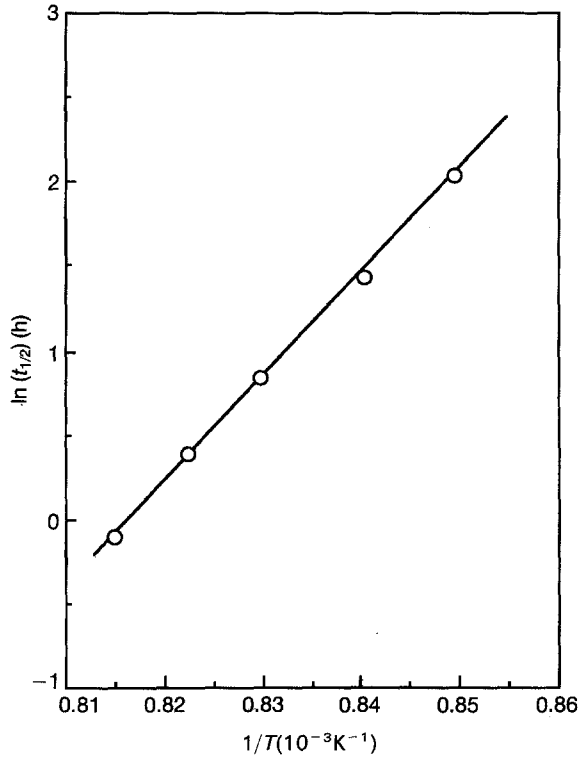

Figure 8 Alternative plot of $\ln(t_{1/2})$ as a function of $1/T$ for determining the activation energy. $E/n = 512\ kJ\ mol^{-1}$.

associated with T_g, and the extrapolated end of T_g, respectively. Activation energy plots for structural relaxation are given in Fig. 13. The data used in the calculation of the activation energies are given in Table X.

TABLE VI Crystallization peak temperatures of cordierite glass determined using DTA and DSC (particle size 600–1000 μm)

Heating rate (K min^{-1})	DTA peak temperature (K)	Heating rate (K min^{-1})	DSC peak temperature (K)
0.67	1265	1.71	1288.0
1.56	1290	3.26	1303.7
3.92	1319	4.81	1322.8
4.65	1325	7.91	1334.2
5.82	1333	9.98	1345.9
7.12	1344	12.05	1354.3
8.11	1347	15.15	1361.0
10.05	1355		

TABLE VII Crystallization peak temperatures of cordierite glass employing DSC (particle size < 45 μm)

Heating rate (K min^{-1})	First crystallization peak (μ-cordierite) (K)	Second crystallization peak (α-cordierite) (K)
1.71	1193.8	1245.7
2.23	1201.4	1252.7
3.78	1210.1	1268.8
4.81	1217.5	1278.1
7.40	1226.9	1290.0
9.98	1232.6	1303.0
12.05	1237.9	1306.6
15.15	1243.5	1315.1

TABLE VIII Crystallization peak temperatures of cordierite glass employing DSC (particle size 45–212 μm)

Heating rate (K min^{-1})	First crystallization peak (μ-cordierite) (K)	Second crystallization peak (α-cordierite) (K)
1.71	1219.3	1276.6
2.23	1222.4	1281.7
3.78	1231.8	1297.2
4.81	1236.6	1305.2
7.40	1247.8	1320.8
9.98	1256.6	1333.3
12.05	1261.5	1340.7
15.15	1267.0	1349.7

6. Discussion

6.1. Crystallization behaviour and characteristic temperatures

For glass of coarse particle size, i.e. 600–1000 μm, a single crystallization exotherm is exhibited, due predominantly to the formation of α-cordierite, also known as high cordierite or indialite. Examination of the characteristic temperatures (Table III) indicates that there is some scatter in the temperature data, suggesting that the glass is not entirely homogeneous. A comparison of the mean values obtained by DTA and DSC shows that, in general the agreement between the different techniques is good, although there is a small discrepancy in some of the data, with the crystallization extrapolated start temperature varying the most (1031 °C by DTA, and 1023 °C by DSC). Small discrepancies of this nature are not, however, unexpected between different measuring systems.

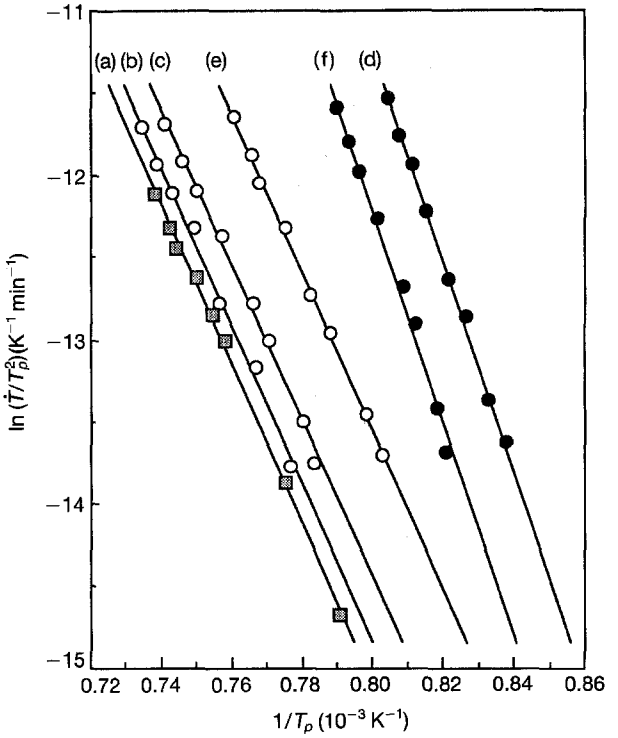

Figure 9 Non-isothermal Kissinger plots constructed from DTA and DSC data for determining the activation energy of crystallization for glass of different particle sizes; (a) 600–1000 μm (DTA); (b) 600–1000 μm (DSC); (c) and (d) 45–212 μm (DSC); (e) and (f) < 45 μm (DSC). See text for details. ▦, DTA/α-cordierite; ○, DSC/α-cordierite; ●, DSC/μ-cordierite. Values of E (kJ mol^{-1}) (a) 404; (b) 400; (c) 395; (d) 542; (e) 399; (f) 532.

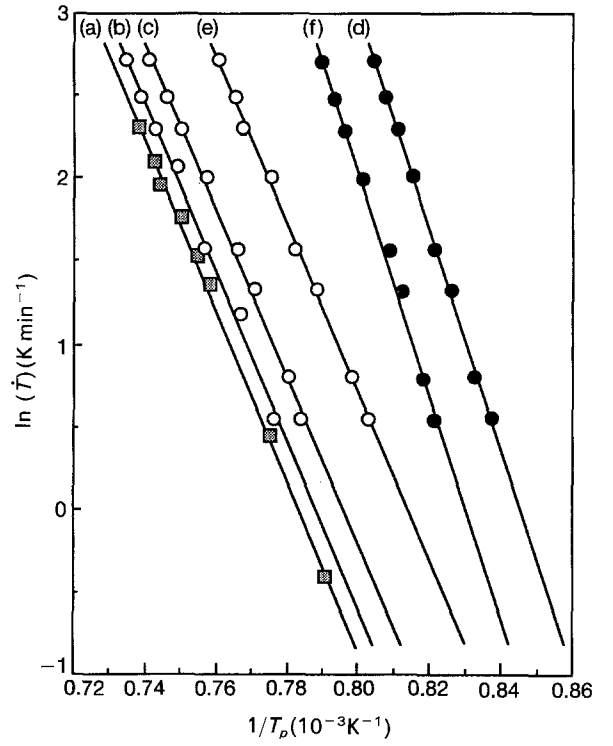

Figure 10 Non-isothermal Ozawa plots constructed from DTA and DSC data for determining the activation energy of crystallization for glass of different particle sizes; (a) 600–1000 μm (DTA); (b) 600–1000 μm (DSC); (c) and (d) 45–212 μm (DSC); (e) and (f) < 45 μm (DSC). See text for details. ▦, DTA/α-cordierite; ○, DSC/α-cordierite; ●, DSC/μ-cordierite. Values of E (kJ mol^{-1}) (a) 426; (b) 423; (c) 416; (d) 562; (e) 420; (f) 553.

TABLE IX Activation energy for crystallization (non-isothermal results by DTA and DSC)

Particle size range (μm)	DTA activation energy ($kJ\,mol^{-1}$)			DSC activation energy ($kJ\,mol^{-1}$)		
	Kissinger	Ozawa	Marseglia	Kissinger	Ozawa	Marseglia
600–1000	404	426	415 (432)[a]	400	423	412 (428)[a]
0–45 (1st peak)	–	–	–	532	553	542 (564)[a]
0–45 (2nd peak)	–	–	–	399	420	410 (426)[a]
45–212 (1st peak)	–	–	–	542	562	552 (574)[a]
45–212 (2nd peak)	–	–	–	395	416	406 (422)[a]

[a] Marseglia value = E/n; values in brackets determined by multiplying this value by n (= 1.04)

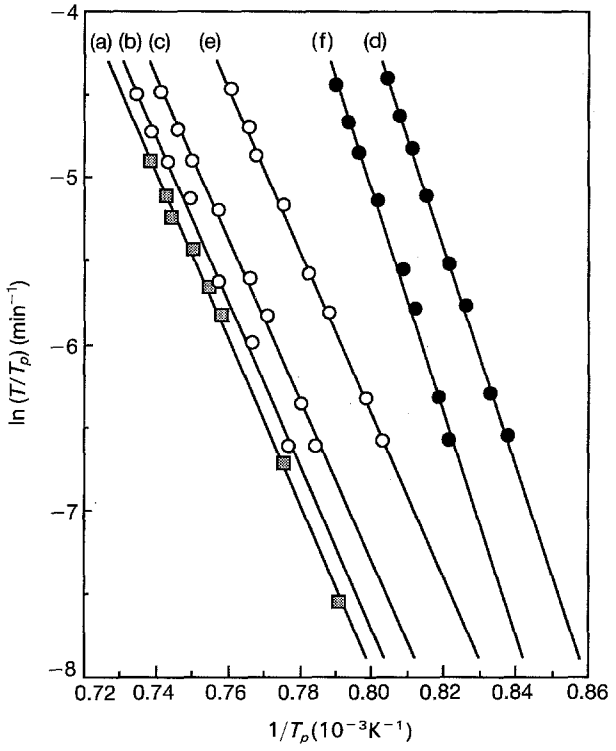

Figure 11 Non-isothermal Marseglia plots constructed from DTA and DSC data for determining the activation energy of crystallization for glass of different particle sizes; (a) 600–1000 μm (DTA); (b) 600–1000 μm (DSC); (c) and (d) 45–212 μm (DSC); (e) and (f) < 45 μm (DSC). See text for details. ▦, DTA/α-cordierite; ○, DSC/α-cordierite; ●, DSC/μ-cordierite. Values of E/n ($kJ\,mol^{-1}$) (a) 415; (b) 412; (c) 406; (d) 552; (e) 410; (f) 542.

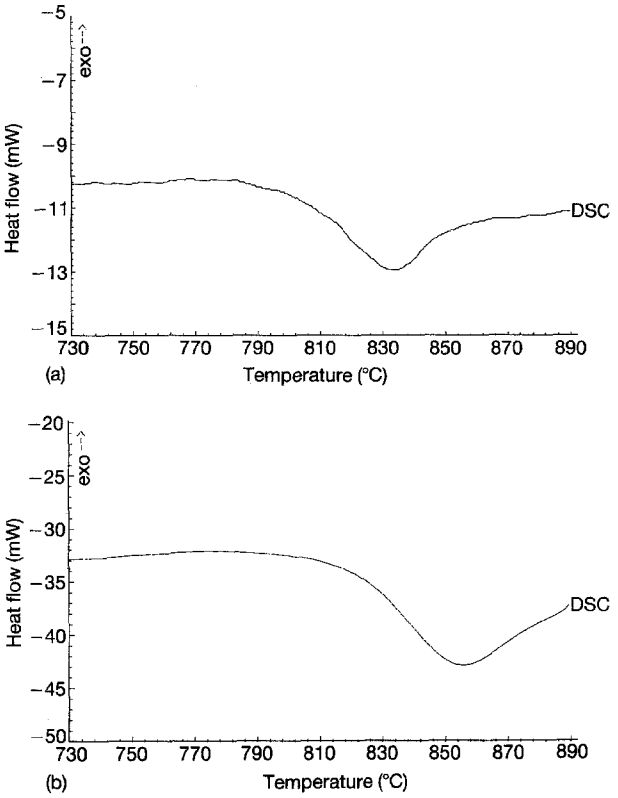

Figure 12 Representative DSC traces showing the glass transition region of cordierite glass. (a) cooling/heating cycle of 10 °C min^{-1}; (b) cooling/heating cycle of 50 °C min^{-1}.

There is a clear influence of particle size on the crystallization behaviour of this glass (Table IV, and Fig. 2). This behaviour is strongly indicative of a predominantly surface nucleation/crystallization mechanism. The emergence of two separate and well-defined crystallization peaks for the smaller size fractions (< 45 μm and 45–212 μm) results from the initial formation at lower temperatures of metastable μ-cordierite (a β-quartz solid solution derivative); this is followed at higher temperatures by conversion to the more stable α-cordierite phase. A similar particle size effect has been noted by other investigators, [4, 24, 26]. The effect of "nucleating" heat-treatments on the crystallization behaviour of the glass indicates that heat-treatment is not effective at promoting bulk crystallization, with the Marotta plot (Fig. 3) showing no evidence for enhanced nucleation. The apparent increase in ΔT at temperatures approaching T_p is due to partial crystallization of the sample during the isothermal hold, as confirmed by the decrease in crystallization enthalpy with increasing hold temperature noted in Fig. 4.

6.2. Activation energies

Traditionally, isothermal methods are employed for determining activation energies. In the present work, a value in the range 532–577 $kJ\,mol^{-1}$ was obtained for the activation energy of crystallization using *isothermal* methods for the glass of coarse particle size, 600–1000 μm, which exhibits a single crystallization exotherm. An average value of 1.04 was noted for the Avrami exponent, n, over the temperature range 904–954 °C, confirming the very strong dependence on surface crystallization.

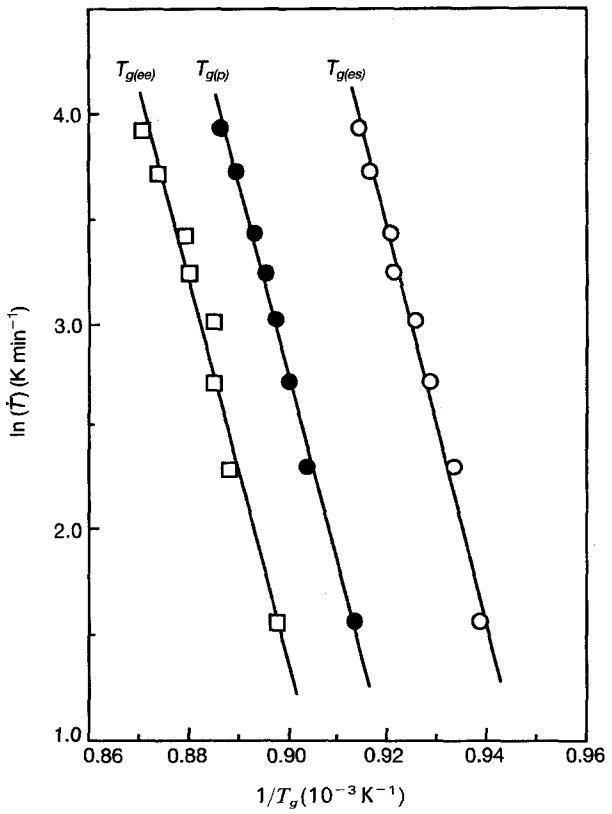

Figure 13 Non-isothermal plots constructed from DSC data for determining the activation energy of structural relaxation associated with the glass transition, E_{relax}, (data for glass of particle size 600–1000 μm); $E_{relax} \approx 766$ kJ mol^{-1}. □, $T_{g(ee)}$; ●, $T_{g(p)}$; ○, $T_{g(es)}$.

TABLE X Glass transition temperature data for cordierite glass determined employing DSC

Heating rate (K min^{-1})	$T_{g(es)}$ (K)	$T_{g(p)}$ (K)	$T_{g(ee)}$ (K)	c
4.81	1065.5	1094.9	1114.4	4.0
9.98	1071.4	1106.3	1127.0	4.2
15.15	1076.8	1110.9	1130.1	4.0
20.32	1080.4	1114.4	1129.9	3.7
25.49	1085.6	1116.7	1136.3	3.8
30.66	1086.1	1119.3	1137.5	3.8
41.00	1090.8	1124.2	1144.7	4.0
51.34	1093.5	1127.9	1148.5	4.0

c = Moynihan parameter [63]

In the case of non-isothermal studies, it is now generally agreed [47–49, 51, 56–62] that use of variable heating rate methods, e.g. the Kissinger [50] or Ozawa [51] methods, for the determination of kinetic data, is strictly applicable only to the derivative thermoanalytical curve. This is most closely satisfied for power-compensated DSC, where the peak of the crystallization exotherm corresponds more closely to the maximum rate of the transformation than is the case when using classical DTA. With DTA (and heat-flux DSC), the maximum rate of transformation is generally expected to occur at some point prior to the peak of the curve. These methods are therefore not necessarily directly applicable for determining activation energies for crystallization of inorganic glasses. It has been shown, however, that the Kissinger or Ozawa methods, when suitably modified (i.e. Equations 6 and 7), may be applied if the predominant crystallization mechanism is known [47–49]. If the precise mechanism of crystallization is known for a given glass system, substitution of the appropriate values for the parameters n and m (Table II) can be made, and a value for the activation energy of crystallization computed accordingly. Equations 6 and 7 reduce to the standard Kissinger or Ozawa equations for the *special* case where surface crystallization predominates. Unfortunately, crystallization occurs for many glasses by simultaneous surface and bulk crystallization, and assignment of unique values for the parameters n and m is not possible. In the present work, however, a stable glass is employed to which no specific nucleating agents have been added. It may be expected, therefore, that surface crystallization effects may predominate for this glass, in which case the standard Kissinger and Ozawa treatments can be applied directly; and, indeed, the predominance of surface crystallization is confirmed both by the value of the Avrami exponent noted above from the isothermal studies, and the non-isothermal Marotta plot. On this basis, determination of the activation energy for crystallization for glass of coarse particle size, 600–1000 μm, using either DTA or heat-flux DSC, gives values which are in remarkably good agreement, in the range 400–432 kJ mol^{-1} depending precisely on which non-isothermal method is employed, as summarized in Table IX.

When employing glass of smaller particle sizes, e.g. < 45 μm and 45–212 μm, the single crystallization exotherm is replaced by two well-defined separate crystallization peaks corresponding to the formation of the μ- and α-cordierite phases, respectively. Determination by DSC of the activation energies of these separate exotherms using the variable heating rate methods yield values for the < 45μm glass of 532–564 kJ mol^{-1} for the first peak (corresponding to μ-cordierite), whilst lower values, i.e. 399–426 kJ mol^{-1}, are noted for the second exotherm (corresponding to α-cordierite). Similar values are noted for glass of particle size 45–212 μm (i.e. 542–574 kJ mol^{-1}; and 395–422 kJ mol^{-1}, respectively). This result indicates that the activation energies for the μ- and α-crystalline phases are insensitive to particle size.

It is interesting to note that the value for the activation energy of the μ-cordierite phase determined using the non-isothermal methods is in close agreement with the value of activation energy determined for coarse (600–1000 μm) powder using the *isothermal* methods. This suggests that crystallization of *coarse* powder during an isothermal hold occurs by initial formation of the μ-cordierite phase, and it is this activation energy that is measured by the isothermal techniques.

Values for the activation energy for crystallization over a wide range, ≈ 270 to 630 kJ mol^{-1}, have been reported for similar cordierite-based glasses. For example, Yuritsin *et al.* [28] determined a value of 628 kJ mol^{-1} for crystallization of μ-cordierite from crystal growth rate data, in fair agreement with the value obtained for μ-cordierite in the present work. On the other hand, a value of ≈ 415 kJ mol^{-1} was

noted by Müller [25], and a value of $\approx 420\,kJ\,mol^{-1}$ was derived by Mora *et al.* [29] for the μ-cordierite phase. Rudolph *et al.* [27] have reported activation energy data determined using both isothermal and non-isothermal methods for a cordierite glass modified by the addition of 4.5 wt% P_2O_5. Isothermal studies based on crystal growth data gave a value for the activation energy of α-cordierite of $469\,kJ\,mol^{-1}$. Lower values were obtained when using variable heating rate methods, i.e. 303 and $325\,kJ\,mol^{-1}$ by the Kissinger and Ozawa methods, respectively. It was found, however, that by employing the crystallization *start* temperature, rather than the peak temperature, higher values were derived, i.e. 473 and $495\,kJ\,mol^{-1}$, respectively. The higher values obtained when using the crystallization start temperature were explained on the basis that the start temperature more accurately reflects the processes occurring during the early stages of crystallization, i.e. most probably μ-cordierite formation. Other values reported for the activation energy of the α phase include $272\,kJ\,mol^{-1}$ for a P_2O_5 modified cordierite glass [9], and $410\,kJ\,mol^{-1}$ for a Y_2O_3–ZrO_2 modified glass [23].

Calculation of the activation energy for structural relaxation around the glass transition using the shift in T_g with cooling/heating rate gave a mean value of $\approx 766\,kJ\,mol^{-1}$ ($777\,kJ\,mol^{-1}$ using the extrapolated start of T_g, $765\,kJ\,mol^{-1}$ using the corresponding peak data, and $756\,kJ\,mol^{-1}$ using the extrapolated end of T_g). This result compares very favourably with a value of $780\,kJ\,mol^{-1}$ reported by Mora *et al.* [29], but is lower than the value of $1004\,kJ\,mol^{-1}$ found by Yuritsin *et al.* [28] for a similar glass. The value determined for the activation energy for structural relaxation is therefore higher than the activation energy for crystallization for the cordierite glass employed in the present work.

Recently, Moynihan has shown empirically [63] that a correlation exists between the width of the glass transition region and the activation energy for structural relaxation around T_g. It was shown, for a wide range of non-metallic inorganic glasses, that the value of the parameter $c = (E_{relax}/R)(1/T_{g_{(es)}} - 1/T_{g_{(ee)}})$, is approximately constant, with a value of 4.8 ± 0.4. In the present work, a mean value for c of 3.9 ± 0.2 was determined for the cordierite glass over a range of cooling/heating cycles, as noted in Table X. This is in fair agreement only, but it should be noted that Moynihan used data for glasses with lower values for T_g than is the case for the cordierite glass used here.

7. Conclusions

This preliminary study of the crystallization behaviour of a cordierite based glass has shown the following:

1. Glass of coarse particle size (e.g. 600 to 1000 μm), exhibits a single crystallization exotherm corresponding to the formation of α-cordierite with a peak temperature centred around 1071–1077 °C (at a standard heating rate of 10 °C min^{-1}). The glass transition temperature for the glass is ≈ 805 °C. Agreement between DTA and DSC was generally good. The heat of crystallization, as determined by DSC, is $361.5 \pm 7.0\,J\,g^{-1}$.

2. A strong dependency of crystallization behaviour on particle size was noted; for example, two crystallization exotherms are resolved for the smaller size fractions examined (< 45 and 45–212 μm), corresponding to the formation of μ-cordierite and α-cordierite phases, respectively. In addition, the α-cordierite peak crystallization temperature increases from 1028 °C to 1088 °C as the particle size increases from < 45 μm to ≈ 3 mm.

3. Isothermal heat-treatment ("nucleation") below the dynamic crystallization temperature, in the range ≈ 860 to 960 °C, causes the glass to undergo partial surface crystallization, with the heat of crystallization decreasing with increasing isothermal hold temperature (i.e. crystallization of the glass occurs rather than the creation of bulk nuclei).

4. For glass of coarse particle size (600–1000 μm), the activation energy for crystallization of the α-cordierite phase determined using non-isothermal methods is in the range 400–432 $kJ\,mol^{-1}$. Agreement between DTA and DSC is excellent.

5. Using glasses of fine particle size (e.g. < 45 μm and 45–212 μm size fractions), activation energies for crystallization of the individual μ-cordierite and α-cordierite phases, determined using non-isothermal methods, are insensitive to particle size and are in the range 532–574 $kJ\,mol^{-1}$ and 399–426 $kJ\,mol^{-1}$, respectively. The value obtained for α-cordierite with glasses of fine particle size is therefore in excellent agreement with the value noted for this phase using the coarse powder.

6. Using isothermal methods a value in the range 532–577 $kJ\,mol^{-1}$ is noted for the activation energy of glass of coarse particle size over the temperature range 904–954 °C. This suggests that the isothermal methods reflect more strongly the *early* crystallization processes and are, therefore, more closely related to the activation energy for the formation of the μ-cordierite phase. An average value for the Avrami exponent, n, of 1.04 was determined, providing additional confirmation for the strong surface crystallization behaviour of this glass.

7. A value for the activation energy for structural relaxation of $\approx 766\,kJ\,mol^{-1}$ was derived at temperatures around the glass transition.

Acknowledgements

This work has been carried out with the support of the Procurement Executive, Ministry of Defence. The work reported forms part of a common research programme performed under the auspices of the Technical Committee on Nucleation, Crystallization and Glass-Ceramics of the International Commission on Glass (TC7 of the ICG).

References

1. P.W. McMILLAN, "Glass-Ceramics", 2nd Edn, (Academic Press, London 1979).

2. T. I. BARRY, L. A. LAY and R. MORRELL, *Proc. Brit. Ceram. Soc.* **22** edited by D. J. Godfrey, British Ceramics Society, (Stoke-on-Trent, 1973), pp. 27–37.
3. I. M. LACHMAN, *Sprechsaal* **119** (1986) 1116.
4. I. UEI, K. INOUE and M. FUKUI, *J. Ceram. Assoc. Japan* **74** (1966) 325 (in Japanese).
5. R.MORRELL, Proc. *Brit. Ceram. Soc.* **28** (1979) 53.
6. E. RABINOVICH, *Advances in Ceramics*, **4** edited by J. H. Simmons, D. R. Uhlmann and G. H. Beall (American Ceramics Society, Columbus, 1982) pp. 327–333.
7. Y. HIROSE, H. DOI and O. KAMIGAITO, *J. Mater. Sci Lett.* **3** (1984) 153.
8. D.R. BRIDGE, D. HOLLAND and P.W. McMILLAN, *Glass Technology* **26** (1985) 286.
9. K. WATANABE and E. A. GIESS, *J. Amer. Ceram. Soc.* **68** (1985) C102.
10. M. A. McCOY and A. H. HEUER, *J. Amer. Ceram. Soc.* **71** (1988) 673.
11. C. I. HELGESSON, *Science of Ceramics*, **8** British Ceramic Society (Stoke-on-Trent, 1979) pp. 347–361.
12. T. RUDOLPH, D. V. SZABÓ, W. PANNHORST, K. -L. WEISSKOPF and G. PETZOW, *Glastech. Berichte* **64** (1991) 218.
13. T. RUDOLPH, K. -L. WEISSKOPF, W. PANNHORST, and G. PETZOW, *Glastech. Berichte* **64** (1991) 305.
14. R. C. C. MONTEIRO, M. M. R. A. LIMA and F. I. F. SILVA in Proceedings of the XVI International Congress on Glass, Madrid, Spain, October, 1992. (Bol. Soc. Esp. Ceram Vid, 31-C, 2, 1992) pp 259–264.
15. M. AWANO, H. TAKAS and Y. KUWAHARA, *J. Amer. Ceram. Soc.* **35** (1992) 2535.
16. S. H. KNICKERBOCKER, A. H. KUMAR and L. W. HERRON, *Bull. Amer. Ceram. Soc.* **72** (1993) 90.
17. K. HAYASHI, T. NISHIYAMA, Y. OKAMOTO and T. NISHIKAWA, *J. Ceram. Soc. Japan* **97** (1989) 328 (in Japanese).
18. A. G. GREGORY and T. J. VEASEY, *J. Mater. Sci.* **6** (1971) 1312.
19. A. G. GREGORY and T. J. VEASEY, *J. Mater. Sci.* **7** (1972) 1327.
20. A. G. GREGORY and T. J. VEASEY, *J. Mater. Sci.* **8** (1973) 324.
21. T. I. BARRY, J. M. COX and R. MORRELL, *J. Mater. Sci.* **13** (1978) 594.
22. K. WATANABE, E. A. GIESS and M. W. SHAFER, *J. Mater. Sci.* **20** (1985) 508.
23. Y. -J. SUE, S-Y. CHEN, H-Y. LU and P. CHEN, *J. Mater. Sci.* **26** (1991) 1699.
24. R. MÜLLER, T. HÜBERT and M. KIRSCH, *Silikattechnik* **37** (1986) 111 (in German).
25. T. MÜLLER, *J. Thermal Anal.* **35** (1989) 823.
26. I. SZABÓ, University of Veszprém, Examination of cordierite glass-ceramics, unpublished report, 1990.
27. T. RUDOLPH, W. PANNHORST and G. PETZOW, *J. Non-Cryst. Solids* **155** (1993) 273.
28. N. S. YURITSIN, V.M. FOKIN, A. M. KALININA and V. N. FILIPOVICH in Proceedings of the XVI International Congress on Glass, Madrid, Spain, October, 1992. (Bol. Soc. Esp. Ceram Vid, 31-C, 5, 1992), pp. 21–26.
29. N. D. MORA, E. C. ZIEMATH and E. D. ZANOTTO in Proceedings of the XVI International Congress on Glass, Madrid, Spain, October, 1992. (Bol. Soc. Esp. Ceram Vid, 31-C, 5, 1992), pp. 117–118.
30. J. O. HILL, (ed), "For better thermal analysis and calorimetry", ICTA Edn, III, 1991.
31. P. MILNER, Netzsch Mastermix Ltd., Walsall, West Midlands, UK. Private communication.
32. R. L. THAKUR and S. THIAGARAJAN, *Glass and Ceramic Bull.* **13** (1966) 33.
33. A. MAROTTA, A. BURI and F. BRANDA, *J. Mater. Sci.* **16** (1981) 341.
34. A. MAROTTA, S. SAIELLO, F. BRANDA and A. BURI, *Verres Réfract.* **35** (1981) 477.
35. S. SAIELLO, F. BRANDA, A. BURI and A. MAROTTA, *Verres Réfract.* **36** (1982) 859.
36. A. MAROTTA, A. BURI, F. BRANDA and S. SAIELLO, *Advances in Ceramics* **4** edited by J. H. Simmons, D. R. Uhlmann and G. H. Beall (American Ceramic Society, Columbus, 1982) pp. 146–152.
37. D. W. HENDERSON, *J. Non-Cryst. Solids* **30** (1979) 301.
38. M. C. WEINBERG, *J. Non-Cryst. Solids* **134** (1991) 116.
39. M. C. WEINBERG, *J. Non-Cryst. Solids* **142** (1992) 126.
40. E. J. MITTEMEIJER, *J. Mater. Sci.* **27** (1992) 3977.
41. W. A. JOHNSON and R.F. MEHL, *Trans. Am. Inst. Min. Metall. Pet. Eng.* **135** (1939) 416.
42. M. AVRAMI, *J. Chem. Phys.* **7** (1939) 1103.
43. M. AVRAMI, *J. Chem. Phys.* **8** (1940) 212.
44. M. AVRAMI, *J. Chem. Phys.* **9** (1941) 177.
45. H. YINNON and D. R. UHLMANN, *J. Non-Cryst. Solids* **54** (1983) 253.
46. M. A. ABEL-RAHIM, M. M. IBRAHIM, M. DONGOL and A. GABER, *J. Mater. Sci.* **27** (1992) 4685.
47. K. MATUSITA, S. SAAKA and Y. MATSUI, *J. Mater. Sci.* **10** (1975) 961.
48. K. MATUSITA and S. SAAKA, *J. Non-Cryst. Solids* **38 & 39** (1980) 741.
49. K. MATUSITA and S. SAAKA, *Bull. Inst. Chem. Res. Kyoto Univ.* **59** (1981) 159.
50. H. E. KISSINGER, *J. Res. Nat. Bur. Standards* **57** (1956) 217.
51. T. OZAWA, *J. Thermal Analysis* **9** (1976) 369.
52. E. A. MARSEGLIA, *J. Non-Cryst. Solids* **41** (1980) 31.
53. C. T. MOYNIHAN, A. J. EASTEAL and J. WILDER, *J. Phys. Chem.* **78** (1974) 2673.
54. C. T. MOYNIHAN, A. J. EASTEAL, M. A. DEBOLT and J. TUCKER, *J. Amer. Ceram. Soc.* **59** (1976) 12.
55. I. AVRAMOV, in Proceedings of the XVI International Congress on Glass, Madrid, Spain, October, 1992. (Bol. Soc. Esp. Ceram Vid, 31-C, 2, 1992), pp. 151–156.
56. R. L. REED, L. WEBER and B. S. GOTTFRIED, *I&EC Fundamentals* **4** (1965) 38.
57. J. H. SHARP, "Differential Thermal Analysis", edited by R. C. Mackenzie (Academic Press, London, 1972) pp. 47–77.
58. E. BAIOCCHI, M. MONTENERO, L. DI SIPIO and A. SOTGUI, *J. Mater. Sci.* **18** (1983) 411.
59. J. SESTAK, *J. Thermal Analysis* **30** (1985) 1223.
60. W. F. HAMMETTER and R. E. LOEHMAN, *J. Amer. Ceram. Soc.* **70** (1987) 577.
61. H. G. WANG, H. HERMAN and X. LUI, *J. Mater. Sci.* **25** (1990) 2339.
62. C. S. RAY, W. HUANG and D. E. DAY, *J. Amer. Ceram. Soc.* **74** (1991) 60.
63. C. T. MOYNIHAN, *J. Amer. Ceram Soc.* **76** (1993) 1081.

Received 7 January
and accepted 5 July 1994